J. Membrane Biol. 134, 93–106 (1993)

The Journal of
Membrane
Biology

Whole Cell K and Cl Currents in Dissociated Eccrine Secretory Coil Cells during Stimulation

Kenzo Sato, Minoru Ohtsuyama, Fusako Sato
Marshall Dermatology Research Laboratories, Department of Dermatology, University of Iowa College of Medicine, Iowa City, Iowa 52242-1181

Received: 18 March 1992/Revised: 25 January 1993

Abstract. Using the whole-cell voltage clamp (to determine the membrane current) and current clamp (to determine membrane potential) methods in conjunction with the nystatin-perforation technique, we studied the effect of methacholine (MCh) and other secretagogues on whole cell K and Cl currents in dissociated rhesus palm eccrine sweat clear cells. Application of MCh by local superfusion induced a net outward current (at a holding potential of −60 mV and a clamp voltage of 0 mV), and a transient hyperpolarization by 5.6 mV, suggesting the stimulation of K currents. The net outward current gradually changed to the inward (presumably Cl) currents over the next 1 to 2 min of continuous MCh stimulation. During this time the membrane potential also changed from hyperpolarization to depolarization. The inward currents were increasingly more activated than outward (presumably K) currents during repeated MCh stimulations so that a net inward current (at −60 mV) was observed after the fourth or fifth MCh stimulation. Ionomycin (10 μM) also activated both inward and outward current. The observed effect of MCh was abolished by reducing extracellular [Ca] to below 1 nM (Ca-free + 1 mM EGTA in the bath). MCh-activated outward currents were inhibited by 5 mM Ba and by 0.1 mM quinidine, although these agents also suppressed the inward currents. Bi-ionic potential measurements indicated that the contribution of Na to the membrane potential was negligible both before and after MCh or ISO (isoproterenol) stimulations and that the observed membrane current was carried mainly by K and Cl. MCh increased the bi-ionic potential by step changes in external K and Cl concentrations, further supporting that MCh-induced outward and inward currents represent K and Cl currents, respectively. Stimulation with ISO or FK (forskolin) resulted in a depolarization by about 55 mV and a net inward (most likely Cl) current independent of external Ca. CT-cAMP mimicked the effects of FK and ISO. The bi-ionic potential, produced by step changes in the external Cl concentration, increased during ISO stimulation, whereas that of K decreased. This indicates that the ISO-induced inward current is due to Cl current and that K currents were unchanged or slightly decreased during stimulation with ISO or 10 μM FK. Both myoepithelial and dark cells responded only to MCh (but not to FK) with a marked depolarization of the membrane potential due to activation of Cl, but not K, currents. We conclude that MCh stimulates Ca-dependent K and Cl currents, whereas ISO stimulates cAMP-dependent Cl currents in eccrine clear cells.

Key words: Eccrine — Sweat — Acetylcholine — Isoproterenol — Channels — Membrane

Introduction

The eccrine secretory coil elaborates nearly isotonic primary fluid in response to Ca-elevating agents such as cholinergic agonists and Ca-ionophores. cAMP-elevating agents such as isoproterenol (ISO), forskolin (FK), and vasoactive intestinal peptide (VIP) also stimulate sweat secretion [12]. Although the secretory coil consists of three types of cells, the clear cell is presumably the main cell type involved in the secretion of salts and water [12]. Secretion of primary sweat generally conforms to a secondary

Correspondence to: K. Sato

active chloride (Cl) transport mechanism [3, 8], where chloride enters the clear cell due to the combined activities of three basolateral membrane transport mechanisms: potassium (K) channels, sodium (Na)-K-2Cl cotransporters, and Na/K pumps. Cl leaves the cell across the luminal membrane, presumably via Cl channels, down the electrochemical potential gradient. This original Na-K-2Cl cotransport model does not require the net outflux of K from the cell because K is assumed to completely recycle across the basolateral membrane via the three basolateral transport mechanisms. Nevertheless, in both salivary acinar cells and eccrine clear cells, cholinergic stimulation results in a net efflux of KCl [1, 13] from the cell and sustained cell shrinkage [2, 19, 20]. In the eccrine clear cell, the net KCl efflux and cell shrinkage are most likely mediated by the stimulation of both K and Cl channels [19], although direct evidence for this thesis is lacking. The mechanism of sweat secretion by cAMP-elevating agents is still poorly understood. During stimulation with isoproterenol (ISO) or other cAMP-elevating agents, a small amount of KCl efflux was noted [13], but it remains unknown whether cAMP stimulates both K and Cl channels or whether it stimulates only Cl channels. It is also unknown whether Na channels are involved in the regulation of sweat secretion.

In the present study, we used the whole-cell voltage/current clamp technique [4] to elucidate how K and Cl currents are regulated by secretagogues. Since cultured cells are not the most ideal model system to study the regulation of membrane events by pharmacological stimulation in native sweat glands [21], we used freshly dissociated rhesus palm eccrine sweat secretory coil cells. Studies from the authors' laboratory have established that the rhesus sweat glands are an ideal model system for human sweat glands [12, 14].

Materials and Methods

Chemicals and Reagents

Unless otherwise noted, all reagents were purchased from Sigma (St. Louis, MO).

Isolation of Secretory Coils

The preparation of isolated rhesus monkey palm sweat glands was essentially the same as described previously [14]. Skin biopsy specimens, approximately 4 × 8 mm, were repeatedly obtained from the palms of 15 adult male monkeys tranquilized with a mixture of Ketalar (Ketamine HCl; Parke-Davis, Morris Plains, NJ) and Innovar (Fentonyl citrate + droperidol; Pitman-Moore, Washington Crossing, NJ). In each monkey, the skin biopsy was done at intervals no shorter than four weeks and the areas of skin adjacent to previous biopsy sites were avoided. The excised tissue was blotted of blood, sliced into several pieces, and immediately washed in several changes of cold (about 10°C) modified Krebs-Ringer bicarbonate solution (KRB) containing (in mM): 125 NaCl, 5 KCl, 1.0 $MgCl_2$, 1.0 $CaCl_2$, 25 $NaHCO_3$, 1.2 NaH_2PO_4, 5.5 glucose, and 20 mg/100 ml bovine serum albumin (BSA). The pH of this medium was 7.48 at 37°C when gassed with a mixture of 5% CO_2/95% O_2. Single sweat glands were isolated under a stereomicroscope using sharp forceps in a dissection chamber kept at 14°C.

Preparation of Dissociated Secretory Coil Cells

Dissociated cells were prepared as described previously [17] with modifications. Briefly, approximately 200 isolated whole sweat glands were first incubated with 0.75 mg/ml type I collagenase in Krebs bicarbonate buffer also containing 10 mM HEPES (HEPES-KRB, titrated to pH 7.48 with NaOH or KOH) for 15 min then thoroughly washed in fresh (collagenase-free) HEPES-KRB. This brief collagenase digestion made the subsequent manual separation of the secretory coils from the ducts considerably easier. Isolated secretory coils (ducts were discarded in the present study) were incubated in KRB containing 0.1 mM Ca, 0.75 mg/ml type I collagenase and 100 μg/ml DNAse I for 5 min at 37°C. The coils were incubated twice for 10 min in 500 μl of Ca- and Mg-free KRB containing 2 mM EGTA. A second enzyme digestion was performed for 30 to 60 min in KRB containing 0.1 mM Ca, 1.25 mg/ml collagenase or 0.125 mg/ml N-tosyl-L-phenylalanine chloromethyl ketone-treated trypsin, penicillin (100 U/ml) and streptomycin (100 μg/ml) mixture, and 100 μg/ml DNAse. The cells were dispersed from the digested glands by repeatedly passing them through a sieve, which was a tungsten grid for electron microscopy (3 mm OD, 100 mesh), epoxy-glued to a disposable plastic pipette, whose tip had been trimmed to 2 mm OD. Dispersed cells were subsequently passed through a finer sieve (200–300 mesh) and centrifuged at 900 × *g* for 2 min. The cells were then suspended in KRB containing 4% bovine albumin. Electron microscopy of the dispersed cells obtained in this way showed more than 60% secretory cells, less than 30% dark cells, and about 10% myoepithelial cells. More than 95% of these cells excluded trypan blue. Myoepithelial cells were readily identified because of their characteristic morphology [19]. Clear cells could be identified with relative ease because of the presence of an autofluorescent lipofuscin granule and cytoplasmic vesicles of varying sizes. Dark cells were the most difficult to identify under phase contrast or Hoffman modulation contrast at 400–600× (Modulation Optics, Greenvale, NY), but they were identified by the lack of lipofuscin granules, a lack of methacholine (MCh)-induced cell shrinkage, and the presence of uniformly sized cytoplasmic dark cell granules [19].

Whole-Cell Voltage/Current Clamp Techniques

Whole-cell current recordings were obtained using the standard method [4] except that the giga-sealed cell membrane patch at the tip of the patch-clamp electrode was perforated by the nystatin method [5]. Sodium borosilicate patch-clamping electrodes had

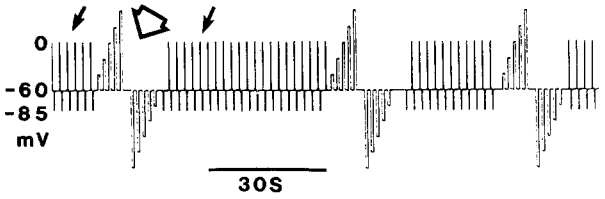

Fig. 1. A representative protocol for clamp voltages used for the whole-cell clamp experiments. Small arrow, alternating clamp voltages at 0 mV and −85 mV of 180 msec duration (every 2 sec) superimposed on the holding potential of −60 mV; large open arrow, step voltages in increments of 20 mV and 800 msec duration. The basis for this protocol is that the Nernst potential is −83.9 mV for K and 0 mV for Cl across the membrane. Because Na (whose Nernst potential is +42.4 mV) conductance is negligible (*see also* Fig. 8), the membrane current is carried mainly by Cl at −85 mV and mainly by K at 0 mV.

a tip resistance of 4–8 MΩ when filled with the pipette solution (containing in mM: 125 KCl, 6.2 Na-HEPES/3.8 HEPES, 0.1 $CaCl_2$/0.2 EGTA, 23 NaCl, 10 glucose, 1 $MgCl_2$, at pH 7.2). The tip of the electrode was first filled with the above solution by capillary action through the tip and the 0.1 mM nystatin containing electrode solution was back-filled. Although Ca and Mg do not readily penetrate nystatin pores and thus [Ca] in the pipette needs no adjustment [5], the electrode solution was chelated to the physiological intracellular concentrations (approximately 100 nM) as a precaution in case Ca-permeable pores were accidentally formed in the patched membrane during sealing by suction. The dissociated cells were placed in a chamber on the stage of a Nikon Diaphot inverted microscope (Nikon, Garden City, NY) thermostated at 30°C and perfused with a constant flow of bath solution from a perfusion pipette. The composition of the bath solution was (in mM): 5 KCl, 141 NaCl, 1 $CaCl_2$, 1 $MgCl_2$, 1 NaH_2PO_4, 6.4 Na-HEPES/3.6 HEPES, 5 glucose, at pH 7.5 (HEPES Ringer). The electrode was mounted on a DC-3K motorized micromanipulator (Stoelting, Wood Dale, IL). An EPC-7 patch-clamp amplifier (List Electronic, Darmstadt, Germany) was used. The output signals were digitized with a PCM-2 (Medical System, Greenvale, NY) and stored on a VHS tape with a VCR recorder (e.g., RCA VR450, Indianapolis, IN) for later replay and analysis. Immediately after forming a giga-seal in a cell-attached configuration and before the membrane was perforated by nystatin (usually achieved within 5 min), the transient capacitance, slow capacitance, and series resistance were compensated for to the maximum allowed by the EPC-7, according to its instruction manual. During all recordings, the series resistance compensation was set at 70–80%. During replay, the current was filtered at 250–500 Hz with an 8-pole low-pass filter (Series 900 filter, Frequency Devices, Haverhill, MA). It was displayed on a Tektronix 5226 oscilloscope (Beaverton, OR) for photographing the current steps and for writing on chart paper with a Gould 2600 pen recorder (Cleveland, OH). For voltage clamping, the membrane potential was changed alternately from the holding potential of −60 to 0 mV (near the Cl equilibrium potential, 180-msec pulses) and to −85 mV (near the K equilibrium potential, small arrow in Fig. 1). Since eccrine clear cells do not have Na conductance [11] (*see* Figs. 8 and 9), the currents at the clamp voltage of 0 and −85 mV largely reflect K and Cl currents, respectively. Whenever appropriate, step voltages in increments of 20 mV from −160 to +40 mV (large arrow in Fig. 1) were injected to construct voltage-current curves. A stable membrane potential of −50 to −80 mV with stable membrane conductance was used as the criterion for adequate formation of nystatin pores in the membrane patch. Drugs were directly applied to the cell from one of seven perfusion pipettes mounted on the side arm of the microscope. We agree with Horn and Marty [5] that the nystatin method minimizes the "run-down" phenomenon (e.g., a gradual or sudden decrease of membrane potential, membrane conductance, and pharmacological responsiveness due most likely to diffusion of cytoplasmic factors into the patch pipette). This was frequently observed when the membrane patch at the electrode tip was disrupted by the suction used in the classical method [4]. In most cells, membrane potential responses were first determined in the (zero) current-clamp mode before the voltage-clamp experiments were started. The membrane potential was monitored thereafter whenever appropriate. If the membrane potential irreversibly decreased to less than −50 mV, the experiment was discontinued. The Donnan potential between the cell interior and the electrode [5] is unknown but could be as much as 3.9 mV, assuming that the total cellular non-Cl anion (phosphate, amino acids, peptides, and proteins that do not cross nystatin pores) concentrations ($= [K]_i + [Na]_i - [Cl]_i$) are about 50 mM [20], where *i* denotes inside the cell. No attempt was made in the present study, however, to correct for such a potential (between the inside of the electrode and the cell interior across the nystatin-perforated cell membrane) because any such Donnan potential would be canceled when the pipette potential was referred to the grounded bath [5]. We did not observe any appreciable cell volume changes after the formation of nystatin pores, indicating that the patched cells effectively regulated the cell volume despite the osmotic disequilibrium due to the Donnan effect. The patched clear cells, however, showed a drastic shrinkage after MCh stimulation as reported in previous studies [19, 20]. The leakage current may be a small fraction of the resting membrane current, as suggested from the extent of the decrease in membrane conductance during the post-MCh stimulation period (*see* Fig. 2*B*), and was thus ignored.

Results

Effects of MCh on Membrane Potential, Membrane Conductance, and K and Cl Currents

Since the clear cell is the major cell type involved in the secretion of salts and water, we focused mainly on clear cells in the present study. The responses of the membrane potential and membrane currents to MCh differed qualitatively and quantitatively in different clear cells and in different cell preparations. However, Fig. 2*A* is an illustrative example of the membrane potential responses to MCh that were most frequently observed. Upon stimulation with 0.3 μM MCh, there was a transient spike of depolarization (small arrow) followed by a short period of hyperpolarization [by 5.6 ± 0.9 mV (mean ± SEM), $n = 43$] with or without oscillation. In general, however, the degree of initial MCh-induced hyperpolarization was dependent on the resting

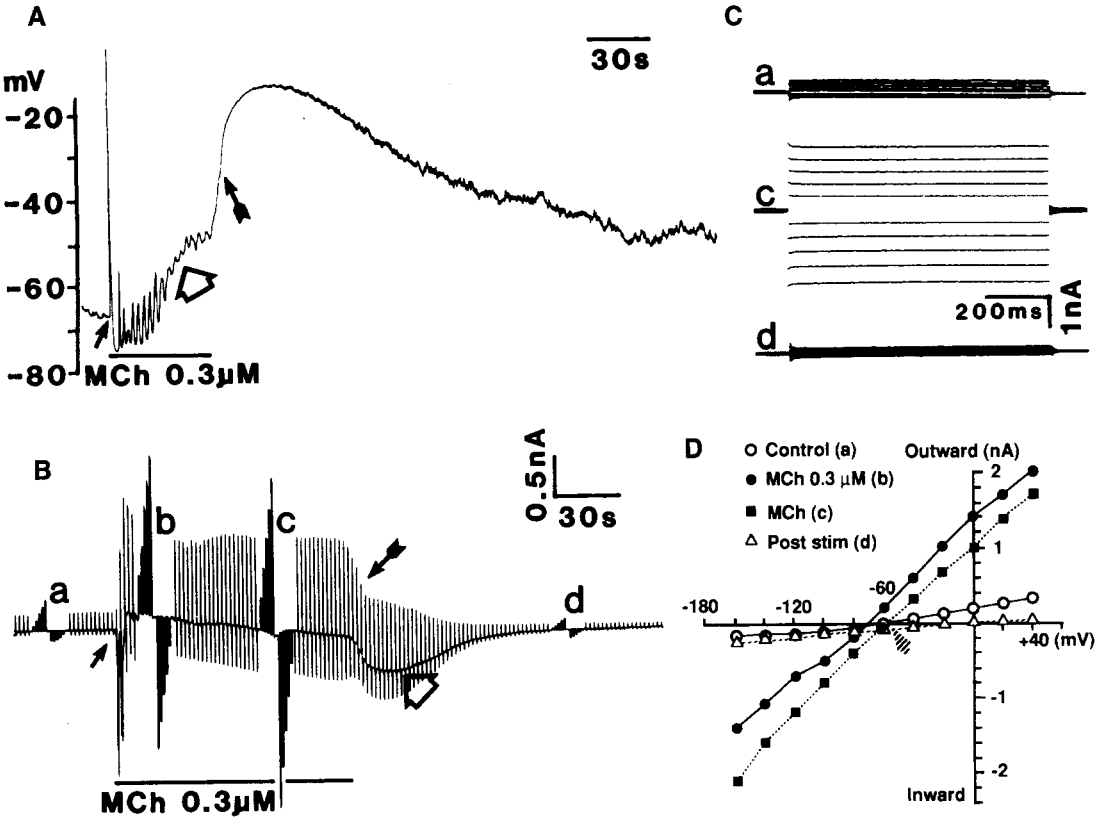

Fig. 2. Effect of MCh on membrane potential as determined by the whole-cell current-clamp technique (*A*) and on membrane current as determined by the whole-cell voltage-clamp method (*B*) in the same eccrine clear cell. In *A:* small short arrow, transient spike of depolarization on stimulation with methacholine (MCh); large open arrow, gradual depolarization during continued stimulation with MCh; small long arrow, rapid depolarization on cessation of MCh stimulation. The washout of the drug was extremely efficient due to continuous perfusion with HEPES Ringer (*see also* Figs. 8 and 9 for the rapid change in the bi-ionic potential by the same perfusion method). In *B: a, b, c,* and *d* are current responses to the incremental clamp voltage protocols (*see* Fig. 1); short small arrow, transient membrane current on stimulation with MCh; long small arrow, rapid decrease in K current on cessation of MCh stimulation; large open arrow, inward drift of membrane current on cessation of MCh stimulation. Note the continued decrease of the membrane current at the right end of the trace which was seen in about a half of the clear cells during the recovery (from prior MCh stimulation) period. The transient capacitance was eliminated during the pen recording with a 15 Hz filter for better illustration of steady-state current levels. (*C*) oscilloscopic sweeps for *a, c,* and *d* in *B*. (*D*) current-voltage (*I-V*) relationship for *a, b, c,* and *d* in *B*. Because the current pulses were nearly steady with time, they were read at their midpoints (at 400 msec) for construction of the *I-V* curves shown in *D*. Throughout the present study, the outward current (positive values plotted on the Y-axis) was defined as the current moving from the cell interior to the bath across the cell membrane. The membrane potential was that of the cell interior with respect to the bath (nA, nanoampere). The duration of the voltage ladder was 800 msec throughout the present study. Since [K] and [Cl] in the cell and the bath are known, and since P_{Na} is negligibly small before and after stimulation (*see* Figs. 8 and 9 for the bi-ionic potential for Na), the P_K/P_{Cl} ratio can be calculated from the constant field equation under the assumptions that the cytosolic ions are readily equilibrated with the pipette solution and that the electrogenic potential is negligible. The P_K/P_{Cl} ratio thus calculated was 30.4 before MCh stimulation (for a PD of −67 mV), 61.3 immediately after MCh stimulation (for a PD of −74 mV), 9.0 during the plateau level of PD during MCh stimulation (for a PD of 49 mV), and 0.9 for the nadir of potential during the post-MCh washout period (for a PD of −14 mV). As shown in Fig. 2*B*, the total membrane conductance (G_{total}) increased about four-fold during MCh stimulation and about three-fold in the post-MCh period. Thus, the relative increases in G_K and G_{Cl} are 8.1-fold and 1.4-fold immediately after MCh stimulation, 5.5-fold and 15.9-fold during the steady state of MCh stimulation, and 1.1-fold and 22.5-fold during the post-MCh potential nadir, respectively. These estimations qualitatively agree with the change in the membrane current shown in Fig. 2*C*.

membrane potential; i.e., the lower the prestimulation membrane potential, the larger the degree of hyperpolarization because the peak membrane potential after MCh only approached −80 mV (*see* subsequent figures for other examples of MCh-induced potential responses). The membrane potential then gradually shifted to a level less negative than the resting level (large open arrow). After the MCh stimulation (and switching to perfusion with HEPES Ringer), the membrane potential then suddenly depolarized further (small long arrow) to as low as −10 to −40 mV but the potential then gradually

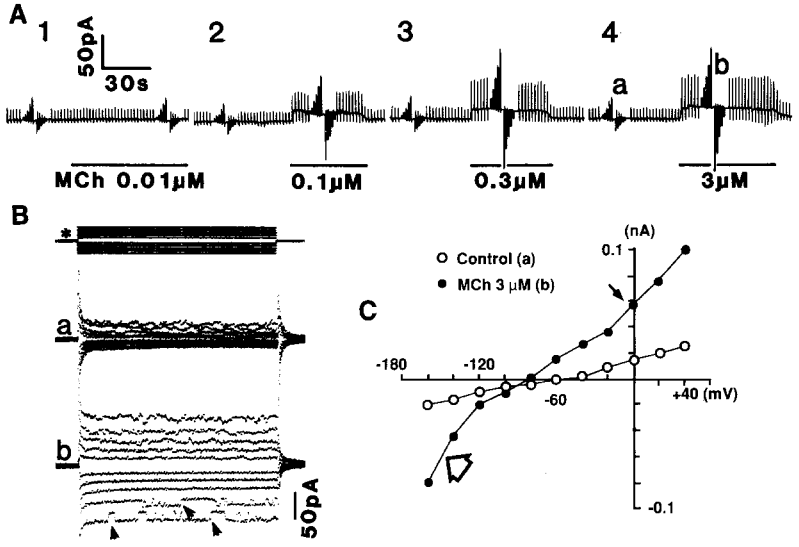

Fig. 3. Response of the membrane current to different doses of MCh in the same cell. Current steps in *4* are shown in *B* and the *I-V* curve in *C*. Small arrowheads in *B* show the transient closure of a 103 pS unitary channel. It may be a Cl channel superimposed on another channel current because the extrapolation of the *I-V* curve for the unitary channel gave a value close to the Cl reversal potential of 0 mV (*not shown*). The anomalous inward rectification in the *I-V* curve *b* in *C* may be due to this unitary Cl channel. The small arrow in *C* shows the increase in the Y-intercept, presumably due to the activation of K conductance.

returned to the prestimulation level within 5 to 7 min. Figure 2*B* shows the whole-cell voltage clamp experiment on the same cell subsequent to the current clamp experiment in Fig. 2*A*. The membrane conductance of a whole cell at rest was relatively constant in each cell (1.6 ± 0.24 nS, range 0.2 to 3.5 nS, $n = 69$). Upon stimulation with MCh, we noted a transient inward current (as shown by downward deflection of current at the holding potential, short arrow in Fig. 2*B*). Although the nature of such a transient spike-like inward current (of a few seconds duration) remains unknown, it corresponded to the transient spike of depolarization in Fig. 2*A*. It was not simply due to a superfusion artifact because other agonists did not produce such a spike. The transient current was followed immediately by an outward current at the holding potential of −60 mV and a marked increase in membrane conductance (from 3 nS before to 18 nS after MCh in Fig. 2*B*), as shown by the larger deflection of current pulses in response to the clamp voltages of 0 mV (the tips of current pulses, largely reflecting K currents) and −85 mV (the bottoms of current pulses, largely reflecting Cl currents). The membrane current at the holding potential, however, gradually drifted toward the inward direction (i.e., downward in the trace) during the continued MCh stimulation. Upon cessation of MCh stimulation, the K current rapidly diminished (long small arrow), resulting in an increase in the inward current at the holding potential (large open arrow in Fig. 2*B*). In more than half the cells studied, the membrane current continued to decrease to well below the prestimulation level during the poststimulation recovery period, although the current returned to the prestimulation level within 5 or 10 min (Fig. 2*B* near *d*). The membrane conductance, however, returned to the prestimulation level within 5 to 7 min after cessation of the stimulation (*not shown*). The response of the membrane current to step voltage pulses was steady over time without time-dependent inactivation or activation (Fig. 2*C*). The steady state current-voltage (*I-V*) curves (Fig. 2*D*) were linear before and after stimulation (without rectification) in most cells studied. MCh stimulation increased the slope of the curve and shifted the reversal potentials (values at the X-intercept) toward the K equilibrium potential of 84 mV (curve *b*, which corresponds to *b* in *B*), indicating that the increase in membrane conductance was most likely due to the increase in K conductance. At *c*, the *I-V* curve shifted to the right, suggesting that Cl conductance was activated on a delayed basis.

Figure 3 shows an illustrative example of MCh dosage *vs.* membrane currents. The current responses increased with MCh concentrations, saturating around 0.3–3 μM ($n = 5$). Since 3 μM MCh required a longer recovery time after each stimulation and the recovery often was not complete, 0.3 μM MCh was preferentially used (unless otherwise noted) in the study, especially when repeated MCh stimulation was required. The observed MCh action was pharmacologically specific because it was completely inhibited by 5 μM atropine ($n = 3$, *not illustrated*). The cell in Fig. 3 also showed a superimposed single channel current at both −140 and −160 mV (arrows in *B*, calculated to be 103 pS); however, this was an infrequent finding. The extrapolation of the single channel current crosses the X-axis at −4 mV (near the Cl equilibrium potential of 0 mV, *not shown*), suggesting that it may be a Cl channel activated by a combination of the negative clamp voltage and MCh. The anomalous inward rectification seen

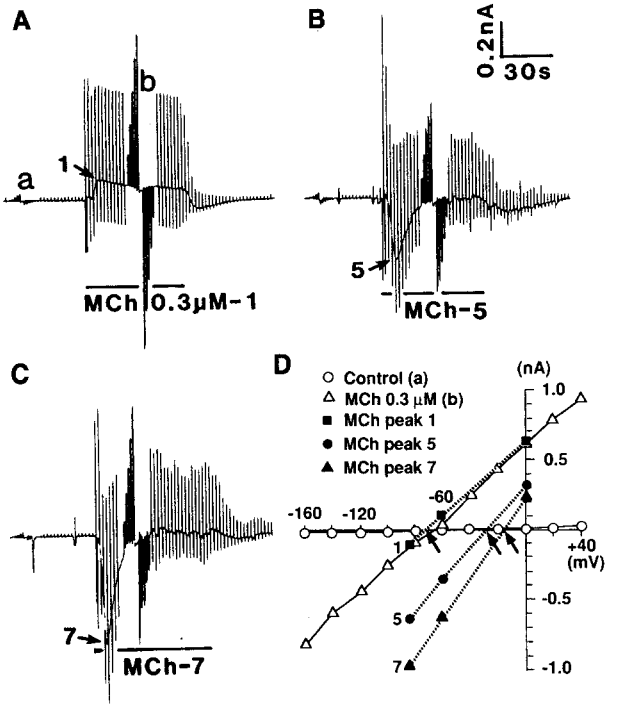

Fig. 4. Effect of repeated MCh stimulation on K and Cl currents. (*A*) the first MCh stimulation; (*B*) the fifth stimulation; (*C*) seventh stimulation. *1*, *5*, and *7* were the peak currents seen at about 10 sec of MCh stimulation. (*D*) shows *I-V* curves for *a*, *b*, and peaks *1*, *5*, and *7*.

in curve *b* in Fig. 3*C* (large open arrow) may be due to activation of this single Cl channel.

Effect of Repeated MCh Stimulation

The current and voltage responses to MCh differ slightly in different clear cells. Furthermore, as suggested in Fig. 2, the MCh-induced K current activation preceded the Cl current activation. Thus, we studied whether K and Cl current responses to MCh remained constant in a given cell or changed with repeated stimulation using three cells. An illustrative example of this study is shown in Fig. 4. The first three repeated MCh stimulations basically yielded a pattern showing a predominantly outward current at the holding potential of −60 mV (Fig. 4*A*). However, the inward current during the initial period of stimulation became more prominent in subsequent episodes of MCh stimulation (Fig. 4*B* shows the fifth MCh stimulation and 4*C* the seventh. Note peaks *1*, *5*, and *7*). *I-V* curves for the three peak responses indicate a gradual shift of the reversal potential toward the Cl equilibrium potential (Fig. 4*D*), indicating that the responsiveness of Cl does change with repeated MCh stimulations.

Effects of Isoproterenol, Forskolin, and cAMP on Membrane Potential and Currents

In contrast to the biphasic nature of the MCh-induced potential and current responses, isoproterenol caused only a depolarization of the membrane potential in a dose-dependent fashion (Fig. 5). The whole cell current at the holding potential (−60 mV) was also directed inward during ISO stimulation (n = 18) and the *I-V* curves shifted toward the Cl equilibrium potential. These observations are consistent with the thesis that ISO-induced depolarization of the membrane potential is due to activation of Cl currents (*see* Fig. 5*C* and *D*). Also note that, as shown in the legend to Fig. 9, the P_K/P_{Cl} ratio dropped from 72.1 in the control to 3.5 during ISO stimulation, reflected by the 74% decrease in G_K after ISO stimulation but the 9.0-fold increase in G_{Cl} during ISO stimulation). Forskolin (FK) mimicked the effects of ISO on membrane potentials and whole cell currents (Fig. 6, n = 8), suggesting that the activation of inward (most likely Cl) current is due to cellular cAMP. This notion is supported by the activation of mainly inward current by 1 mM CT [8-(4-chlorophenylthio)]-cAMP + 0.2 mM IBMX (Fig. 7). The slow time course of the response to CT-cAMP may be due to its slow rate of penetration into the cell. The *I-V* curves in Fig. 7*D* suggest that K currents were also activated during stimulation. Activation of K currents, in addition to that of Cl currents, during stimulation with cAMP-elevating agents was not a constant finding, however. The K current tended to become activated, but to a minor extent, during prolonged stimulation with 50 mM FK (three out of seven clear cells, *not illustrated*) or when 0.2 mM IBMX was added to ISO (two out of five cells, *not illustrated*).

Bi-Ionic Potentials during Ionic Replacement in the Bath

The foregoing discussion is based on the premise that Na does not contribute to the whole cell current and thus the inward current is carried largely by Cl and the outward current mainly by K. To examine such a thesis, bi-ionic potentials were determined by quickly replacing the extracellular K, Cl, and Na with less permeable ionic substitutes. As shown in Fig. 8*A* and *B*, the magnitude of depolarization due to the 10-fold change in the medium [K] increased from a mean of 42 before stimulation to 51 mV after MCh stimulation. These ΔPD (potential differences) correspond to the apparent ion-dependent partial potential ratios (T_i) [18] of about 0.70 and 0.85, respectively. In contrast, during reduction of the Cl

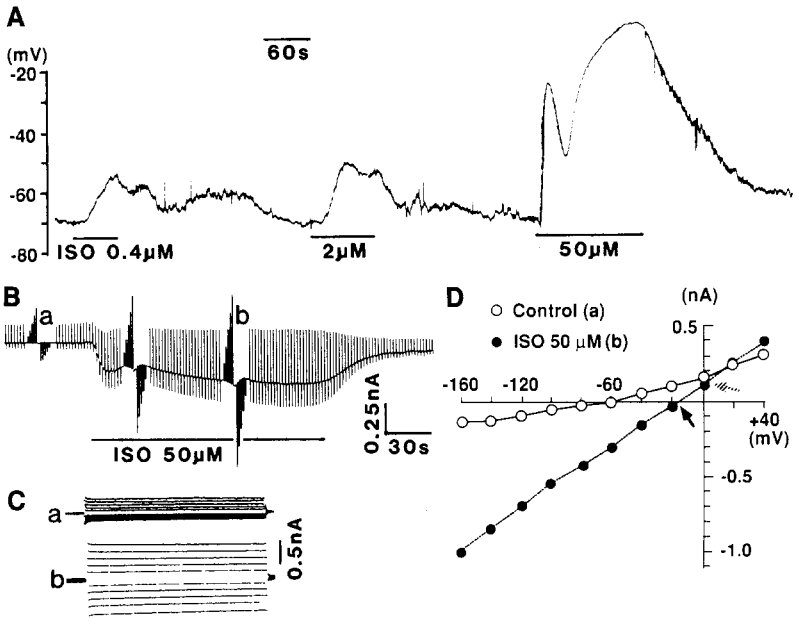

Fig. 5. Effect of isoproterenol (ISO) on the membrane potential (*A*) and whole cell current (*B*) in a clear cell. Note the dose-dependent depolarization of the membrane potential in *A*. The mean magnitude of depolarization was 9.8 ± 0.48, 21.3 ± 3.1, and 56.0 ± 4.7 mV (n = 5, mean ± SEM) for 0.4, 2, and 50 μM ISO, respectively. ISO (50 μM) was mainly used for the whole-cell clamp studies (*B*). In the present study, phosphodiesterase inhibitors such as theophylline and isobutylmethyl xanthine (IBMX) were not used in combination with ISO or forskolin to avoid any nonspecific effects these inhibitors may have. (*C*) Oscillograph of the current responses to the voltage ladders from *a* (before) and *b* (during stimulation with ISO) shown in *B*. (*D*) *I-V* curves for *a* and *b* showing the steady current responses. The shaded arrow indicates a small decrease in the Y-intercept (i.e., no increase in the K current), whereas the rightward shift of the curve (filled arrow) indicates an increase in the Cl current.

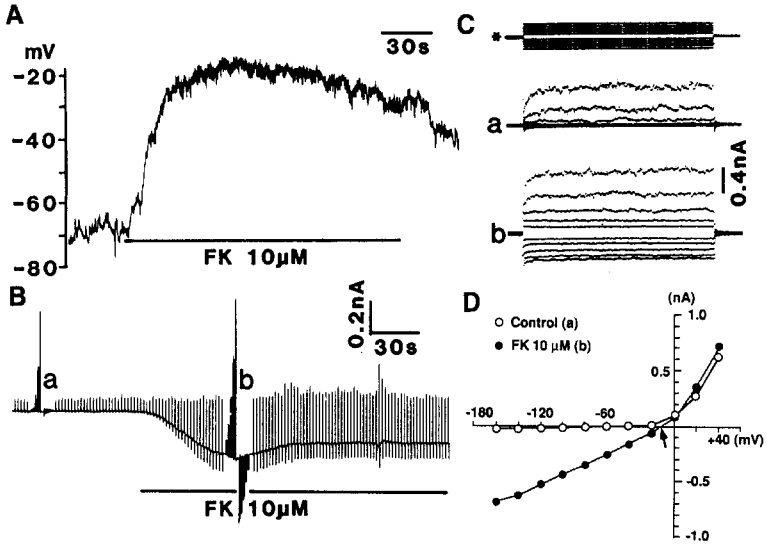

Fig. 6. Effect of forskolin (FK) on the membrane potential (*A*) and whole cell currents (*B* and *C*) in a clear cell. The upper trace in *C* (*) is the voltage ladder. (*D*) *I-V* curves for *a* (control) and *b* (during stimulation with FK) shown in *B*. Note the rightward shift of the curve during FK stimulation (filled arrow). The maximum depolarization was 54.6 ± 2.8 mV for 10 mM FK (n = 8).

concentrations from 150 to 19 mM, ΔPD increased from zero to 16 mV, yielding the apparent T_i values of 0 and 0.30, respectively. Reduction of medium Na concentrations from 152 to 35 mM caused no change in the membrane potential before or during stimulation with MCh (*see* Fig. 8*D*). As shown in Fig. 9, the 10-fold increase in medium [K] brought about the ΔPD of 44 and 39 mV before and during stimulation with 50 μM ISO (which correspond to the apparent T_i values of 0.73 and 0.65, respectively). Again, the ΔPD for Na replacement remained unchanged during ISO stimulation. However, the ΔPD for the reduction of the medium [Cl] from 150 to 19 mM caused a depolarization of 0 before and 22 mV during stimulation with ISO (which correspond to the apparent T_i values of 0 and 0.41, respectively). The change in $[Na]_o$ thus had no effect on PD, providing indirect evidence that Na conductance is negligible before and after stimulation and that the membrane currents are carried largely by K and Cl.

Role of Ca on the Effects of MCh and ISO

Cholinergic stimulation is associated with an increase in cytosolic [Ca] in sweat clear cells [17]. MCh-induced, but not ISO-induced, sweat secretion

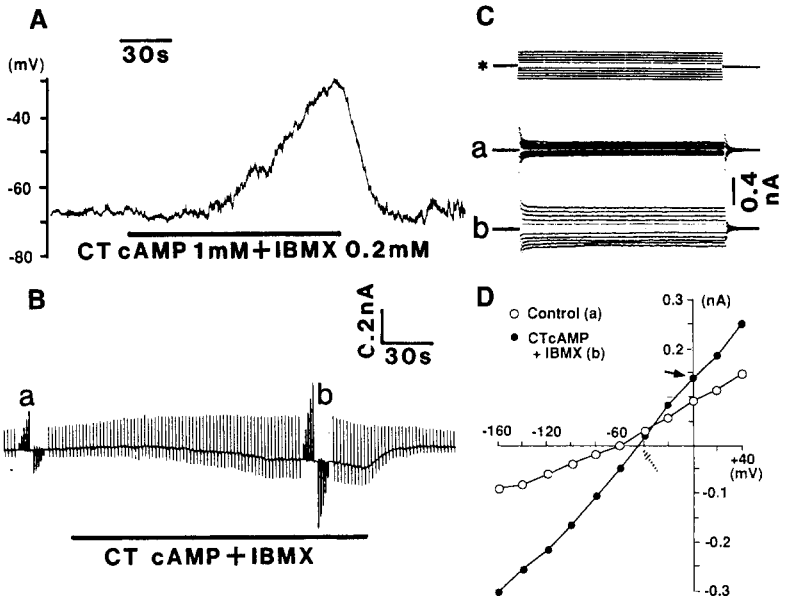

Fig. 7. Effect of CT-cAMP on the membrane potential and whole cell current in a clear cell. (*A*) membrane potential; (*B*) whole cell current; (*C*) voltage (*) and current ladders *a* (before) and *b* (during cAMP stimulation); (*D*) *I-V* curves for *a* and *b*. The CT-cAMP curve shifted to the right (shaded arrow) but the Y-intercept also increased, suggesting the simultaneous activation of K currents. An illustrative experiment from three similar studies. CT-cAMP without IBMX (isobutylmethyl xanthine) had no effect (n = 2, *not illustrated*); 0.2 mM IBMX alone had no effect on the membrane potential or currents (n = 3).

and K efflux in vitro are also dependent on extracellular Ca [13, 15]. Thus, the effect of buffering cytosolic [Ca] to the nanomolar range (by adding 1 mM EGTA to a nominally Ca-free electrode solution) was first tested on MCh-induced whole cell current using the conventional whole-cell clamp method (without using nystatin pores). MCh-induced activation was either absent or markedly reduced in all the cells studied (n = 12, *not illustrated*), although the "run down" phenomenon frequently encountered with the classical patch-clamping method [4, 5] precluded the specificity of the observation. The effect of low extracellular [Ca] was then studied with the nystatin method (as used throughout the study). As shown in Fig. 10, the reduction of extracellular Ca (<1 nM) had no effect on ISO-induced depolarization of the membrane potential (Fig. 10*A*) or ISO-induced activation of Cl currents (Fig. 10*B*). However, repeated stimulations with MCh in a Ca-free (<1 nM) medium abolished the effect of MCh (Fig. 10*C*). To study the effect of the increased cytosolic [Ca] on membrane potential and currents, we then examined the effect of 10 μM ionomycin (n = 4). Ionomycin (10 μM) was comparable to 3 μM MCh in increasing cytosolic [Ca], stimulating sweat secretion in vitro (*unpublished data*), and inducing cell shrinkage [19]. As can be seen in Fig. 11*A*, ionomycin drastically depolarized the membrane potential without initially causing the transient hyperpolarization that can be seen frequently with MCh. The time course of ionomycin-induced whole cell currents, however, resembled that seen after repeated stimulation with MCh (*see* Fig. 4*C*), i.e., an initial surge of inward current with delayed activation of the outward current. In fact, the *I-V* curves indicate that both Cl and K currents were activated by ionomycin (Fig. 11*D*).

Effects of Barium and Quinidine on MCh-induced Cl and K Currents

Since the preceding observations suggested that cytosolic Ca plays a key role in the activation of K currents during MCh stimulation, we studied the effects of barium (Ba) and quinidine—putative inhibitors of Ca-dependent K channels [6], on MCh-activated K currents. As shown in Fig. 12, Ba significantly inhibited MCh-induced K current as shown by the decrease in the Y-intercept (filled arrow in Fig. 12*B*). It is puzzling, however, that Ba also shifted the MCh-curve to the right (shaded arrow in Fig. 12*B*), suggesting that Cl currents were also inhibited. Interestingly, quinidine (0.1 mM) behaved similarly to Ba (n = 4, *not illustrated*). No further studies were performed to elucidate the mechanism of the observed simultaneous inhibition of K and Cl channels by Ba and quinidine.

Whole-Cell Current/Voltage Clamp Studies of Myoepithelial and Dark Cells

Myoepithelial cells can be readily identified because of their large size and characteristic morphology [19]. All five myoepithelial cells studied showed depolarization by MCh (3 cells with 3 μM and 2 cells with 0.3 μM MCh). Despite the dramatic depolariz-

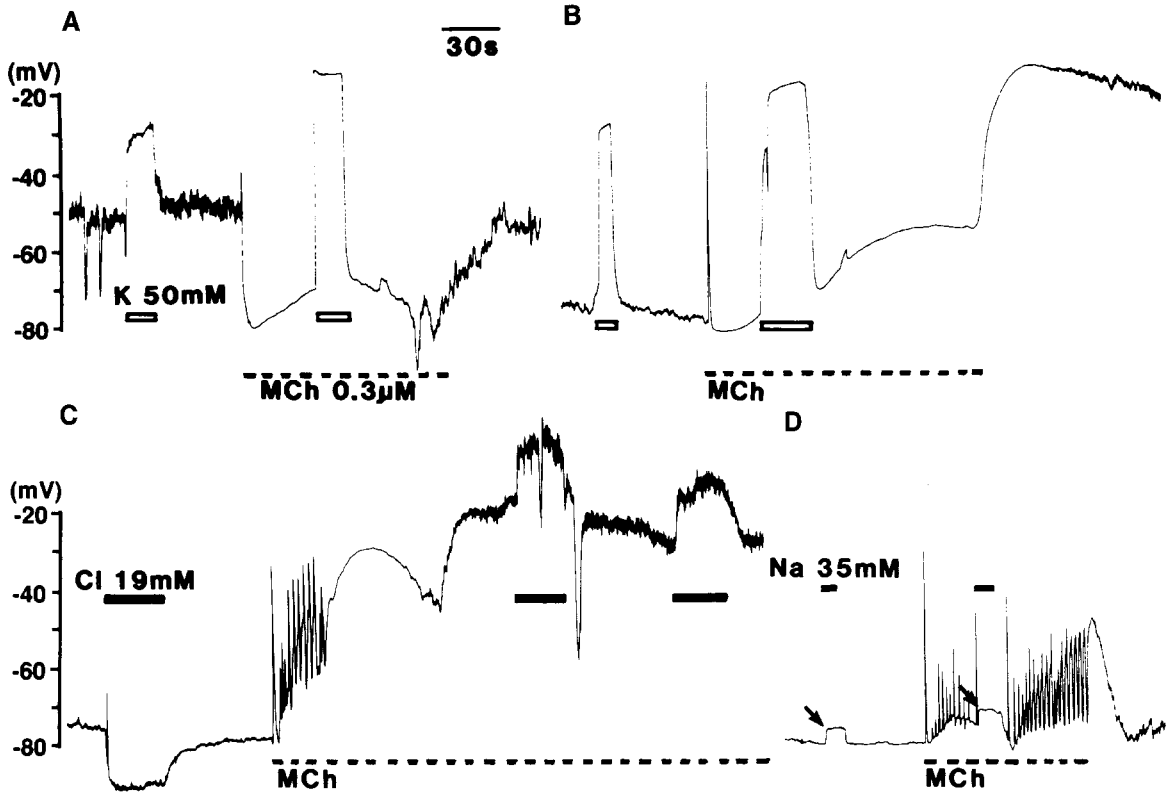

Fig. 8. Bi-ionic potentials for K, Cl, and Na before and during MCh stimulation in eccrine clear cells (illustrative experiments). K in the perfusates was replaced by Na, Cl replaced by methylsulfate, and Na by N-methyl-D-glucamine (pH adjusted with HCl). During stimulation with MCh, 50 mM K (K50) in HEPES Ringer (or other perfusates) contained 0.3 μM MCh. K50-induced depolarization was 41.9 ± 4.8 mV during the resting period and 50.6 ± 2.4 mV during 0.3 μM MCh stimulation (n = 6). (*A–B*) illustrative examples of K50-induced depolarization. (*C*) bi-ionic potential due to reduction of the medium [Cl] from 150 to 19 mM. The observed hyperpolarization during Cl replacement before MCh was mainly due to a liquid junction potential (−5.8 mV as determined directly between the free-flowing 3 M KCl electrode and the perfusate) and thus Cl19-induced depolarization was practically zero. In contrast, during MCh stimulation, ΔPD increased to 16 ± 1.3 mV (corrected for liquid junction potential) (n = 4). (*D*) reduction of [Na] from 152 to 35 mM (arrows) had no effect on the membrane potential (after being corrected for the estimated liquid junction potential of 5 mV) before and during MCh stimulation (n = 4).

ing response to MCh, the myoepithelial cells failed to respond to FK. Their membrane conductances were much lower than those of clear cells both before [0.32 ± 0.05 (n = 5) *vs.* 2.89 ± 0.46 (n = 20) nS] and during MCh stimulation [0.46 ± 0.11 (n = 5) *vs.* 37.7 ± 8.5 (n = 20) nS between 0 and −85 mV]. *I-V* curves (Fig. 13*D*) show that both K and Cl currents were activated by MCh but the latter were activated to a greater extent as suggested by the depolarization of the membrane potential. Since dark cells were difficult to identify under the optical system used for the voltage-clamp studies (i.e., Hoffman modulation contrast), a group of cells that lacked lipofuscin granules, contained cytoplasmic (dark cell) granules of uniform size, and showed no cell shrinkage upon MCh stimulation [19] were operationally defined as dark cells. As shown in Fig. 14, these cells showed drastic depolarization upon MCh stimulation yet failed to respond to FK. The *I-V* curves show that the initial surge of inward current was entirely due to activation of Cl currents (Fig. 14*B* and *C*). Thus, although we are without positive identification of these cells as dark cells, they are distinct from clear cells by a combination of electrophysiological, morphological, and functional characteristics.

Discussion

Although the responsiveness of human and monkey eccrine sweat glands to cholinergic and adrenergic agents has been well studied, the detailed membrane events associated with pharmacological stimulations have remained poorly understood [12]. Conventional glass microelectrode studies provided only

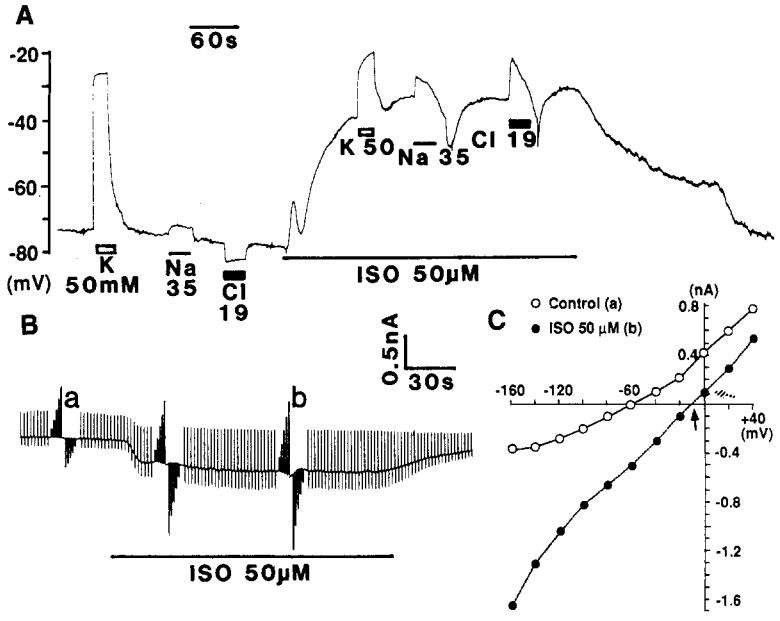

Fig. 9. Bi-ionic potentials for K, Cl, and Na before and during stimulation with 50 μM ISO in a clear cell. (*A*) potential responses to K, Na, and Cl replacement before and during stimulation with ISO. (*B*) same cell, subsequent to *A*, showing ISO-induced inward current. (*C*) *I-V* curves for *a* and *b* in *B*. The shaded arrow shows the decrease in the Y-intercept, suggesting a decrease in K currents. The filled arrow shows the rightward shift of the curve, suggesting an increase in Cl conductance. ΔPD for K replacement was 43.5 ± 3.9 and 18.6 ± 2.8 mV before and during ISO stimulation, respectively (n = 4). ΔPD for Na replacement was 0.11 ± 0.03 and 0.12 ± 0.01 (corrected for the liquid junction potential) before and during ISO stimulation, respectively (n = 3). ΔPD for the reduction of Cl from 150 to 19 mM was 0 and 22 ± 2.1 mV, respectively (n = 3). The P_K/P_{Cl} ratio, calculated from the potential trace in Fig. 9*A* using the constant field equation, was 72.1 before ISO stimulation (for a PD of −72 mV) but dropped to 3.5 during ISO stimulation (for a PD of −33 mV). The relative changes in G_K and G_{Cl} were calculated to be 0.74-fold and 9.0-fold, respectively, during the nadir of ISO stimulation in Fig. 9*B*.

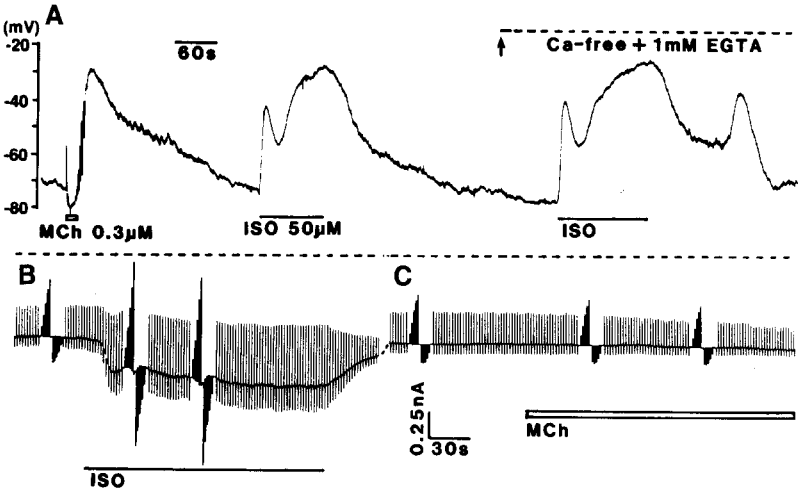

Fig. 10. Effect of Ca-free medium on the membrane potential and membrane currents during stimulation with ISO and MCh in a clear cell. Three other experiments had similar results. ISO-induced depolarization was unchanged after the removal of extracellular Ca (*A*). The cell continued to be superfused with Ca-free (<1 nM) HEPES Ringer when a second ISO stimulation failed to detect a significant decrease in inward current (*B*). Note that the observed ISO-induced inward current is very similar to those observed in other cells bathed in normal Ringer solution (e.g., Figs. 5 and 9). Subsequent repeated stimulations with MCh in the Ca-free Ringer abolished the MCh-induced depolarization (*not illustrated*) and activation of membrane currents (*C*).

limited information on the electrophysiological responses of sweat secretory cells [11, 16]. Using the whole-cell voltage/current clamp method [4] combined with the nystatin-perforation technique [5], we succeeded in obtaining stable membrane potentials and whole cell currents from single cells to study the effects of various pharmacological stimulations. Using freshly dissociated rhesus eccrine clear cells, we observed that stimulation with methacholine (MCh) resulted in activation of both K and Cl currents. In most clear cells, MCh initially stimulated mainly K currents producing a net outward current (at the holding potential of −60 mV) regardless of the MCh dose. Concurrently, the membrane potential was hyperpolarized (after an initial transient spike of depolarization). Within 30 sec to 1 min after beginning MCh stimulation, Cl currents were increasingly activated so that the initial net outward current changed to a net inward current (at the holding potential of −60 mV). This caused the membrane potential to depolarize to a level less negative than the prestimulation level. After stopping the MCh

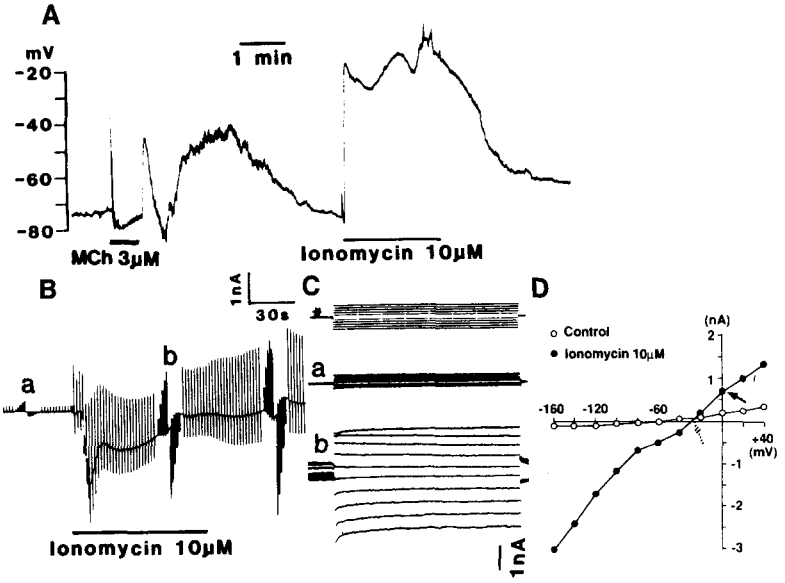

Fig. 11. Effect of a Ca-ionophore, ionomycin, on the membrane potential (*A*) and currents (*B*) in a clear cell. (*C*) Oscillograph of the membrane current in response to the voltage ladder (*) in increments of 20 mV. *a* and *b* in *C* correspond to those in *B* and *D*. Note the increase in both K (filled arrow in *D*) and Cl (shaded arrow in *D*) currents during stimulation with ionomycin. In all four cells studied, ionomycin caused similar potential (depolarization by 44.1 ± 5.8 mV) and current responses.

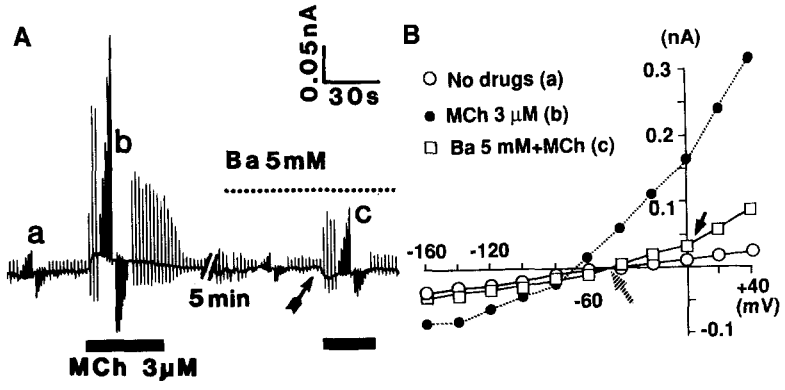

Fig. 12. Inhibition of MCh-induced K and Cl currents by Ba^{2+}. Four other experiments had similar results. Ba (5 mM) drastically inhibited the MCh-stimulated K current (as shown by the filled arrow in *B*). Ba^{2+} also shifted the MCh curve to the right (shaded arrow), indicating that the Cl current was also decreased (n = 5).

stimulation, K currents subsided first, temporarily leaving Cl currents more dominant, further stimulating inward current and causing a marked depolarization of the membrane potential. The poststimulation inward current subsided within a few minutes, but in about half the cells studied, the whole-cell clamp current continued to decrease to well below the prestimulation level during the post-MCh stimulation washout period. Repeated MCh stimulation during this "refractory period" resulted in markedly obtunded responsiveness to MCh (*not shown*). Thus, care needed to be taken to ensure the complete recovery of the membrane potential and the whole cell current before a second pharmacological stimulation was applied.

Upon repeated MCh stimulations, however, activation of Cl currents became more dominant so that MCh stimulation caused initial net inward current even though K currents were simultaneously activated. Interestingly, stimulation with 10 μM ionomycin, a calcium ionophore, also caused an initial net inward current and initial marked depolarization of the membrane potential, although K currents were also activated subsequently. The activation of K and Cl currents by MCh is pharmacologically specific and is most likely mediated by cytosolic Ca because the effects of MCh were abolished by atropine, by excessive chelation of cytosolic Ca with EGTA (using the conventional method of disrupting the membrane patch by suction), and by the removal of extracellular Ca. K current activated during MCh stimulation may be due to Ca-dependent K channels [6, 7] because they were inhibited by barium and quinidine. It is puzzling, however, that these putative inhibitors of K channels also inhibited Cl currents. It remains to be studied whether such anomalous observations reflect unknown nonspecific effects or the "functional cross talk" between Cl and K channels. The qualitative differences in the current and potential responses between MCh and

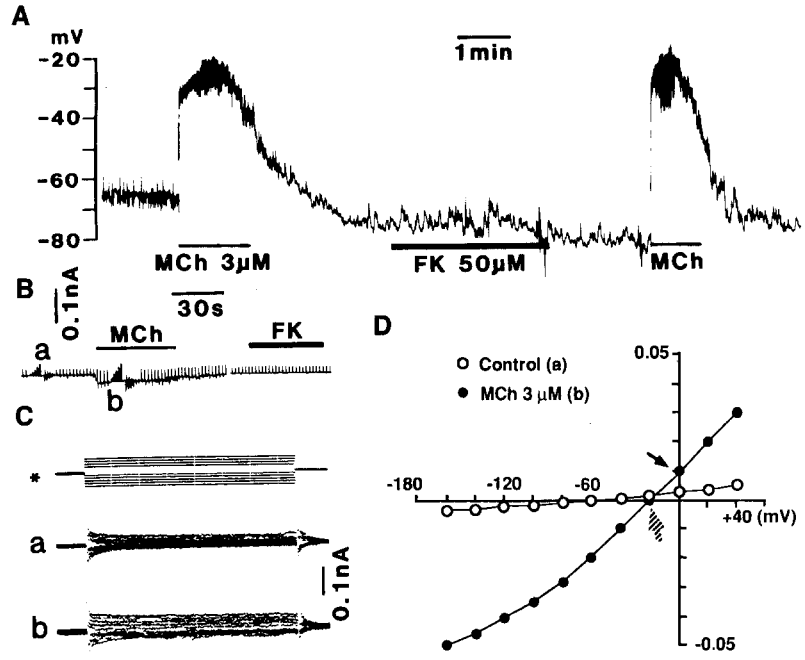

Fig. 13. Effects of MCh and FK on the membrane potential (*A*) and whole cell current (*B*) in myoepithelial cells. (*C*) Oscillographic pictures of membrane currents in response to clamp voltage ladders. (*D*) *I-V* curves for *a* (before) and *b* (during MCh stimulation) indicated in *B*.

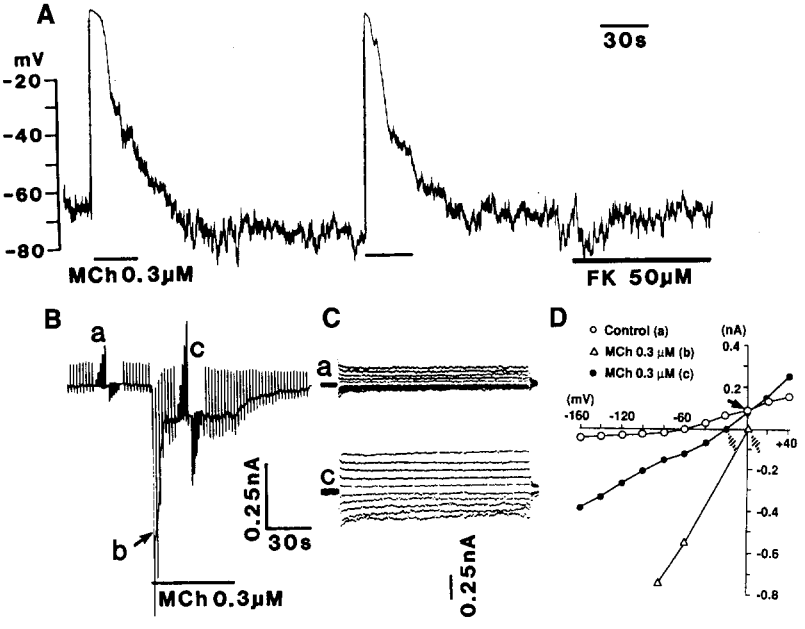

Fig. 14. Effect of MCh and FK on the membrane potential (*A*) and whole cell current (*B*) in cells lacking lipofuscin granules and MCh-induced cell shrinkage. In the absence of positive identification, these cells were operationally defined as dark cells. In (*D*) the *I-V* curve from the MCh transient (*b* in *B*) was also illustrated (triangles in *D*).

ionomycin should also be investigated in the future. The present study also demonstrated that only K and Cl currents were activated during pharmacological stimulations in clear cells and that the contribution of Na to the membrane current was negligible both before and after stimulations. The lack of Na current before and during pharmacological stimulation supports the basic premise of the study that the outward current is carried largely by K and the inward current by Cl.

During stimulation with ISO (isoproterenol) or FK (forskolin), the membrane potential depolarized by about 55 mV and was associated with a net inward whole cell current. ISO-induced depolarization was dose dependent. The effects of ISO on activation of the Cl current may be most likely due to cAMP (or the effect of the cAMP cascade) because CT-cAMP, a membrane permeable derivative of cAMP, also stimulated Cl currents. Also, FK mimicked the effect of ISO. K currents were unchanged or slightly decreased during stimulation with ISO or 10 μM FK, indicating that the decrease in K conductance may

partly contribute to the marked depolarization of the membrane potential in some cells. A minor activation of K current was, however, observed in a small number of cells when they were stimulated by 50 μM FK (on a delayed basis) or by a combination of cAMP-elevating agents and IBMX, suggesting that the observed K current activation in the minority of cells may be due to a nonspecific effect of IBMX or to prolonged exposure to the excessive cytoplasmic levels of cAMP.

Myoepithelial cells have a much lower membrane conductance than clear cells and responded only to MCh (but not to FK) with a marked depolarization of the membrane potential due to activation of Cl, but not K, currents. Although dark cells cannot be positively identified under the optical system used in the present voltage-clamping experiment, we selected a group of cells with the morphological and functional features of dark cells, i.e., the lack of lipofuscin granules, presence of small uniform cytoplasmic granules (presumably dark cell granules), and absence of MCh-induced cell shrinkage [19]. These cells also responded only to MCh (but not to FK) with a marked depolarization of the membrane potential due to stimulated Cl, but not K, currents. Given that there is a subset of cells with features of both clear and dark cells [12] (suggesting that one cell type may derive from the other), strict separation of dark cells from clear cells may not be warranted. Nevertheless, the present study provided evidence that dark cells may behave differently from clear cells in their electrophysiological responses to MCh and cAMP-elevating agents.

The present whole-cell voltage/current clamp study successfully produced basic information on the activation of membrane currents during stimulation with MCh and cAMP-elevating agents. The results are consistent with the notion that cholinergic stimulation of the clear cell is associated with stimulation of Ca-dependent K and Cl channels, whereas stimulation with cAMP-elevating agents is associated with the stimulation of cAMP-dependent, relatively Ca-insensitive, Cl channels. In this respect, it is of interest to note that eccrine clear cells behave somewhat similarly to the acinar cells of rodent salivary and lacrimal glands [1, 6, 7, 9, 10]. It remains to be studied, however, why K and Cl currents in the eccrine sweat gland cells are regulated differently in different cells during the time course of (MCh) stimulation or by repeated stimulations. It is also unknown whether or not only calcium is involved in MCh-induced stimulation of K and Cl channels because the effect of ionomycin was somewhat different from that of MCh. The characteristics of individual channels must also be elucidated. The present work has thus provided the basis for further studies on the regulation of membrane channels by pharmacological agents, the pivotal event during sweat secretion.

This paper has been supported in part by NIH grants DK 27857, AR 25339 and a Cystic Fibrosis Foundation Grant G124. Sue Cavallin helped in preparation of the manuscript.

References

1. Cook, D.I., Young, J.A. 1989. Fluid and electrolyte secretion by salivary glands. *In:* The Handbook of Physiology. The Gastrointestinal System III. S.G. Schultz and J.G. Forte, editors, pp 1–23. American Physiological Society, Bethesda, MD
2. Foskett, J.K., Melvin, J.E. 1989. Activation of salivary secretion: coupling of cell volume and $[Ca^{2+}]_i$ in single cells. *Science* **24(4912):**1582–1585
3. Frizzell, R.A., Field, M., Schultz, S.G. 1979. Sodium-coupled chloride transport by epithelial tissues. *Am. J. Physiol.* **236(1):**F1–F8
4. Hamill, O.P., Marty, A., Neher, E., Sakmann, B., Sigworth, F.J. 1981. Improved patch-clamp techniques for high-resolution current recording from cells and cell-free membrane patches. *Pfluegers Arch.* **391:**85–100
5. Horn, R., Marty, A. 1988. Muscarinic activation of ionic current measured by a new whole cell recording method. *J. Gen. Physiol.* **92:**145–159
6. Iwatsuki, N., Petersen, O.H. 1985. Inhibition of Ca^{2+} activated K^+ channels in pig pancreatic acinar cells by Ba^{2+}, Ca^{2+}, quinine, and quinidine. *Biochim. Biophys. Acta* **819:**249–257
7. Marty, A., Tan, Y.P., Trautmann, A. 1984. Three types of calcium-dependent channel in rat lacrimal glands. *J. Physiol.* **357:**293–325
8. O'Grady, S.M., Palfrey, H.C., Field, M. 1987. Characteristics and functions of Na-K-Cl cotransport in epithelial tissues. *Am. J. Physiol.* **253:**C177–C192
9. Petersen, O.H. 1992. Stimulus-secretion coupling: cytoplasmic calcium signal and the control of ion channels in exocrine acinar cells. *J. Physiol.* **448:**1–51
10. Petersen, O.H., Gallacher, D.V. 1988. Electrophysiology of pancreatic and salivary acinar cells. *Annu. Rev. Physiol.* **50:**65–80
11. Sato, K. 1986. Effect of methacholine on ionic permeability of basal membrane of the eccrine secretory cell. *Pfluegers Arch.* **407(Suppl 2):**S100–S106
12. Sato, K., Kang, W.H., Saga, K., Sato, K.T. 1989. Biology of sweat glands and their disorders. I: Normal sweat gland function. *J. Amer. Acad. Derm.* **20**(4):537–565
13. Sato, K.T., Saga, K., Ohtsuyama, M., Takemura, T., Kang, W.H., Suzuki, Y., Sato, K. 1991. Movement of cellular ions during stimulation with isoproterenol in simian eccrine clear cells. *Am. J. Physiol.* **261:**R87–93
14. Sato, K., and Sato, F. 1981. Pharmacologic responsiveness of isolated single eccrine sweat glands. *Am. J. Physiol.* **240:**R44–R51
15. Sato, K., Sato, F. 1981. Role of Ca^{2+} in cholinergic and adrenergic mechanism of eccrine sweat secretion. *Am. J. Physiol.* **241:**C113–C120
16. Sato, K., Sato, F. 1982. Transepithelial p.d. during Sr^{2+}-

induced spontaneous sweat secretion. *Am. J. Physiol.* **242(11):**C360–C365
17. Sato, K., Sato, F. 1988. Relationship between Quin 2-determined cytosolic [Ca^{2+}] and sweat secretion. *Am. J. Physiol.* **254:**C310–C317
18. Strickholm, A., Wallin, B.C. 1981. Relative ion permeabilities in the crayfish giant axon determined from rapid external ion changes. *J. Gen. Physiol.* **50:**1929–1953
19. Suzuki, Y., Ohtsuyama, M., Samman, G., Sato, F., Sato, K. 1991. Ionic basis of methacholine-induced shrinkage of dissociated eccrine clear cells. *J. Membrane Biol.* **123:**33–41
20. Takemura, T., Sato, F., Saga, K., Suzuki, Y., Sato, K. 1991. Intracellular ion concentrations and cell volume decrease during cholinergic stimulation of eccrine secretory coil cells. *J. Membrane Biol.* **119:**211–219
21. Yokozeki, H., Saga, K., Sato, F., Sato, K. 1990. Pharmacological responsiveness of dissociated native and cultured eccrine secretory coil cells. *Am. J. Physiol.* **258:**R1355–R1362